Development of Pneumatically Driven Tensegrity Manipulator without Mechanical Springs

doi: https://doi.org/10.1109/IROS47612.2022.9982208

Development of Pneumatically Driven Tensegrity Manipulator without Mechanical Springs

Yuhei Yoshimitsu[1], Kenta Tsukamoto[1] and Shuhei Ikemoto[1,2]

***Abstract*— This paper reports a tensegrity manipulator driven by 40 pneumatic cylinders without mechanical springs. In general, tensegrity robots use mechanical springs to achieve a stable/curved tensegrity structure, and this is true even when a component extends/retracts with an actuator. The stiffness of the mechanical spring should be high to increase the stiffness of the entire structure and improve the control response, but low to deform the structure. This fact means that the introduction of mechanical springs causes serious trade-offs in its design and control. In this study, we use pneumatic actuators not only for active deformation but also for passive. In this paper, we introduce the design and control system and then show the difference in response characteristics between the case with and without a spring, demonstrating the importance of the approach without a mechanical spring.**

I. INTRODUCTION

In a broad sense, tensegrity is a structure that keeps three-dimensional shape by tensile forces, and in a narrow sense, it refers to such a structure in which there is no contact between rigid bodies and no bending moment in rigid bodies. In [1], tensegrity with k rigid-body contacts is defined as *class* k tensegrity. Therefore, tensegrity in the narrow sense is called *class* 1 tensegrity. Tensegrity is known as a structure that is lightweight, strong, and rich in design, and these features are salient for the class 1.

In robotic applications of tensegrity, the class 1 tensegrity has been first used for mobile robots. So far, multiple gait patterns, e.g. crawling gait[2], [3] and rolling gait[4], [5], and their control/learning methods, e.g. evolutionary algorithm[6] and deep reinforcement learning[7], have been widely studied. In these studies, the class 1 tensegrity was used to deform the overall shape of robots with fewer actuators than members. Generally speaking, tensegrity is a prestressed structure, and the stresses carried by the members are not uniquely determined. Therefore, when an actuator actively applies force to one member, it is difficult to calculate which other members need to be deformed and by how much to obtain a change in the overall shape. Mechanical springs are commonly used to ease this difficulty in implementing of tensegrity robots driven by non-backdrivable motors. However, this leads to many trade-offs among agility, deformation amount, size/weight of the robot, etc.

*This work was supported by JSPS KAKENHI Grant Numbers 19K0285, 19H01122, and 21H03524.

[1]Y. Yoshimitsu, K. Tsukamoto, and S. Ikemoto are with Graduate School of Life Science and Systems Engineering, Kyushu Institute of Technology, 2-4 Hibikino, Wakamatsu, Kitakyushu, Fukuoka, Japan. ikemoto@brain.kyutech.ac.jp

[2]S. Ikemoto is with the Research Center for Neuromporphic AI Hardware, Kyushu Institute of Technology

Fig. 1. The developed tensegrity manipulator. This robot is based on class 1 tensegrity and consists of 20 struts, 40 pneumatic cylinders, and 40 stiff cables. The height and mass are approximately 1.2 [m] and 3.5 [kg], respectively.

On the other hand, class k tensegrity has been commonly used for tensegrity robots other than mobile robots, e.g. jumping robot[8], robot spine[9], [10], and manipulator[11], [12], [13]. The explicit joint structures between rigid bodies facilitate the use of small rotary actuators and the design of the shape and deformation of the tensegrity. However, joint structures and rigid bodies with complex shapes that bear bending moments reduce the advantages of tensegrity. In contrast, we are developing a tensegrity manipulator using class 1 tensegrity toward achieving extremely high redundancy seen in animals and humans. In [14], we have proposed the design method of the tensegrity manipulator and evaluated the manipulator that arm-like tensegrity consists of 20 struts and can be deformed by 20 pneumatic cylinders and 20 springs. However, even using backdrivable pneumatic actuators, the stiffness of the spring poses a trade-off between the output/agility and deformation amount.

In this paper, we present a manipulator based on class 1 tensegrity consisting of 20 struts, 40 pneumatic cylinders, and 40 stiff cables, as shown in Fig.1. Because no mechanical springs are used, all deformation of the tensegrity is caused by active and passive displacements of the pneumatic cylinders. The passive displacement of the pneumatic cylinders behaves like a mechanical spring whose stiffness changes according to the internal pressure, which is expected to significantly improve the performance from the tensegrity manipulator in [14].

This paper is organized as follows: Section II explains the design and control system of the developed tensegrity

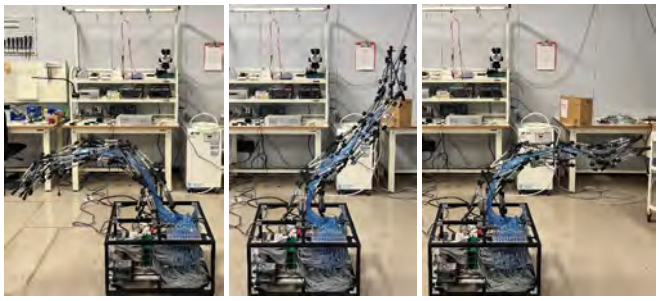

Fig. 2. Samples postures of the developed tensegrity manipulator. It can take various continuously bending postures depending on pneumatic cylinders' internal pressure patterns.

Fig. 3. Mechanical parts consisting of the developed tensegrity manipulator. No.1, No.2, No.3, and No.4 indicate strut, stiff cable, pneumatic cylinders, and connectors, respectively.

manipulator. Section III shows setups and results of experiments conducted for evaluating improvements achieved by the developed robot. We will discuss the results and future work in Section IV and conclude in Section V.

II. DEVELOPED TENSEGRITY MANIPULATOR

Fig.2 shows different continuously bending postures that the developed robot can realize. Compared to the tensegrity manipulator using mechanical springs introduced in our previous study[14], the new manipulator has an improved range of motion and posture variation. As shown in these pictures, the strut ends of the manipulator are attached to the top of a black aluminum frame box, in which 40 pneumatic pressure control valves and the control boards are included, via ball joints. Power and compressed air are supplied by 100 V AC and an external compressor (SLP-07EED, ANEST IWATA). In the following subsections, the mechanical design, control system, and motion performance are described separately.

A. Mechanical Design

Thanks to the use of class 1 tensegrity, the developed tensegrity manipulator can be constructed from a small number of mechanical parts. Briefly speaking, only struts, stiff cables, pneumatic cylinders, and connectors that connect the cables to the others form the structure. Fig.3 shows those fundamental parts constituting the tensegrity manipulator. The strut is a CFRP pipe with an inner diameter of 4 [mm], an outer diameter of 5 [mm], and a length of 300 [mm]. The

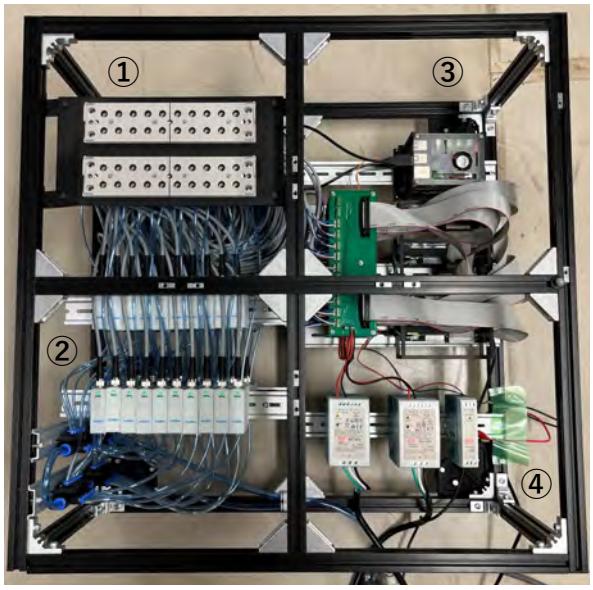

Fig. 4. The control system of the developed tensegrity manipulator. No.1, No.2, No.3, and No.4 indicate air connectors, pressure control valves, control boards for valves, and power supplies, respectively.

stiff cable is a Kevlar braid line with a tensile strength of over 1000 [N]. The developed tensegrity manipulator uses only one type of strut and stiff cable. On the other hand, it employs two types of pneumatic cylinders with the same stroke length of 45 [mm] and inner diameters of 16 [mm] and 10 [mm]. The high power and heavy cylinders are used at the base, and low power and light cylinders are used at the tip. The connectors were designed to easily connect the stiff cable to other parts and were fabricated with a 3D printer (Mark Two, Markforged).

The developed manipulator has an arm-like tensegrity constituted from five simple tensegrity modules. Thus, it looks to having five segments as appeared in Fig.1 and Fig.2. In particular, each segment in the developed manipulator has eight pneumatic cylinders, so there are 40 pneumatic cylinders in total. See [14] for the design rule that the developed tensegrity manipulator employed and how to use these parts in the structure.

B. Control System

The developed tensegrity manipulator takes a posture corresponding to the equilibrium point of the pneumatic cylinder's tensile force. Therefore, the pressure control of pneumatic cylinders is the fundamental function of the control system of the developed tensegrity manipulator. Adjusting target pressures of all pneumatic cylinders, the control system conducts feed-forward posture control. Fig.4 shows the overview of the control system mounted in the black aluminum frame box. The connectors of the air tubes appear in the upper left of this figure. One connector connects 20 tubes at once. In the lower-left, 40 pressure control valves (VEAB, FESTO) are installed. This valve receives a desired pressure signal and provides an actual pressure value. The control boards in the upper right manage these

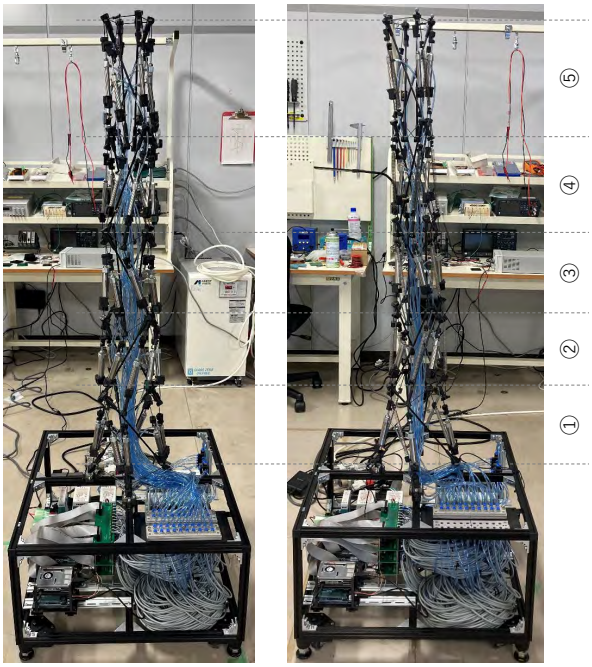

Fig. 5. Tensegrity manipulators with 20 and 40 pneumatic cylinders. Left: Tensegrity manipulators with 40 pneumatic cylinders. The overall structure consists of five segments, and each segment has eight pneumatic cylinders. Right: Tensegrity manipulators with 20 pneumatic cylinders. It also consists of five segments, but each segment has four pneumatic cylinders and four mechanical springs.

signals to control the developed tensegrity manipulator. It consists of five Arduino Mega boards and amplifier shields and one Ubuntu 20.04 LTS installed Raspberry Pi 4. One of the file Arduino Mega boards communicates with the Raspberry Pi 4 by RS-232C and communicates with the other four Arduino Mega boards by I2C at the same time. These four Arduino Mega have amplifier shields and controls 10 pressure control valves based on commands sent from the Raspberry Pi 4 via the one Arduino Mega board. The Raspberry Pi 4 has ROS (ROS2 Foxy) installed, and desired and actual pressures are exchanged with other nodes via the topic communication. The lower right shows power supplies for valves and controllers.

III. EXPERIMENT

Fig.5 shows the developed tensegrity manipulator employing 40 pneumatic cylinders (left) and the tensegrity manipulator in [14] that uses 20 pneumatic cylinders and 20 springs (right).

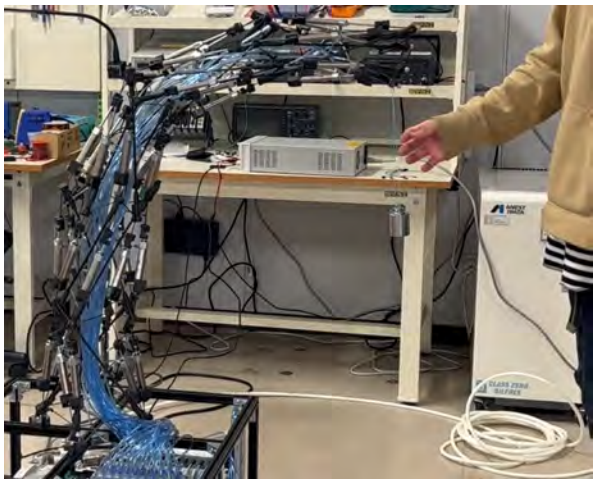

Fig. 6. The overview of loading experiment. Pneumatic cylinders in the segment 1 and 2 are equally pressurized, and the others make the manipulator bending. By suspending a 500 [g] weight at the tip, the relationship between pressures in the segment 1 and 2 and displacement is evaluated.

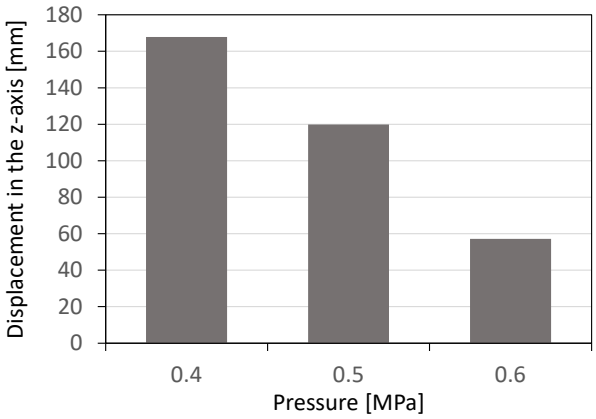

Fig. 7. The result of loading experiment. Pressures for pneumatic cylinders in the segment 1 and 2 clearly vary the stiffness of the developed tensegrity manipulator.

As shown in the figure, both of these manipulators have five segments. There is no major difference other than whether four of the eight vertical tension members in each segment use mechanical springs or all eight use pneumatic cylinders. To evaluate the improvements achieved by replacing mechanical springs with pneumatic cylinders to eliminate springs from the structure, we conducted two types of experiments. In this section, we describe the setups and results of the two experiments.

A. Variable stiffness characteristics

At first, we evaluate the characteristics of the variable stiffness of the developed tensegrity manipulator and compare the results with those obtained using a mechanical spring presented in [14]. Fig.6 shows the overview of loading experiment. In this experiment, the same bending posture is made at different pressures, and a 500 [g] weight is suspended from the tip to evaluate the displacement in the vertical axis. To generate the bending posture, we configured

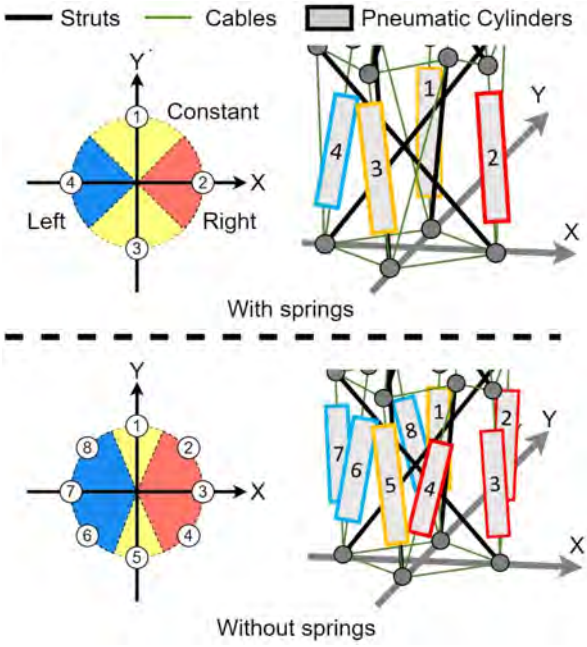

Fig. 8. The schematic of swing motion generation. pneumatic cylinders in each layer are categorized into three groups. Pneumatic cylinders in the same group receive the same desired pressure value. For the "Left" and "Right" groups, sinusoidal desired pressure values with opposite phases are given. It varies between 0.3 and 0.6 [MPa]. The "Constant" group gets a constant pressure of 0.45 [MPa].

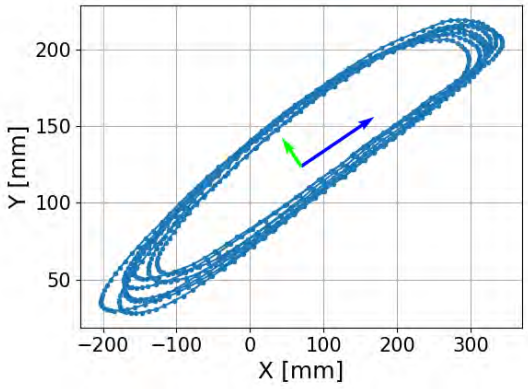

Fig. 9. A trajectory of manipulator's tip during swing motions measured by a motion capture system. Depending on the frequency of the desired pressure values, the tip draws ellipsoidal trajectories in the X-Y plane. Principal Component Analysis (PCA) is applied to a trajectory, and the principal component is deemed as the output of the swing motion.

pressures to pneumatic cylinders in segments 3, 4, and 5, and the others are equally pressurized to aim to change the stiffness. In the experiments, the desired pressures applied to segments 1 and 2 were set to 0.4, 0.5, and 0.6 [MPa] to overcome the friction in pneumatic cylinders.

Fig.7 shows the results of loading experiment. This graph clearly shows the variable stiffness of the developed tensegrity manipulator. In addition, it observes that the pressures given to segments 1 and 2 almost linearly change the stiffness. Although a rigorous evaluation is not possible due to differences in the methods for posture generation and

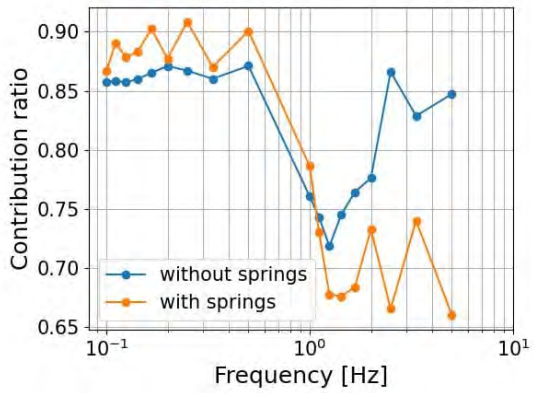

Fig. 10. Changes in the contribution ratio of principal component 1. In the manipulator with springs, an increase in the input frequency monotonically decreases the contribution of principal component 1. In the developed manipulator that does not use springs, the contribution ratio of principal component 1 decreases once and then recovers corresponding to increase in the input frequency.

displacement measurement, the results of using a mechanical spring shown in [14] shows that a load of 130[g] results in a displacement of approximately 200-500 mm. Because the mechanical springs impose certain flexibility on the manipulator that cannot be removed, it is difficult to reduce the displacement by adjusting the desired pressures. On the other hand, the developed tensegrity manipulator has no mechanical springs, so the displacement can be reduced to approximately 60 mm for a load of 500 [g] by adjusting the target pressure. The results of this experiment show that the manipulator without springs is clearly stiffer and will be able to hold heavy objects over 500 [g]. Note that larger displacements can be easily observed by reducing the pressures in segments 1 and 2 than that was observed in [14].

B. Frequency response characteristics

In the next, we evaluate the characteristics of the frequency response of the developed tensegrity manipulator and the manipulator presented in [14]. In particular, in this section, we evaluate the relationship between the frequency of swing motions of tensegrity manipulators connecting for the frequency of the desired pressure changes.

Fig.8 depicts the schematic of desired pressure generation for swing motions. Tensegrity manipulators with and without springs have four and eight pneumatic cylinders in each segment. To generate desired pressure values for these cylinders, we categorize them into three groups, namely "Left", "Right", and "Constant" groups, and the same group receives the same desired pressure values. The "Constant" group receives a constant desired pressure value of 0.45 [MPa]. It only contributes stabilize swing motions. The "Left" and "Right" groups receive sinusoidal desired pressure values that vary between 0.3 and 0.6 [MPa] with opposite phases. It indicates that a sinusoidal wave governs all desired pressure values and that the frequency is the sole parameter.

Fig.9 shows trajectories of the manipulator's tip during

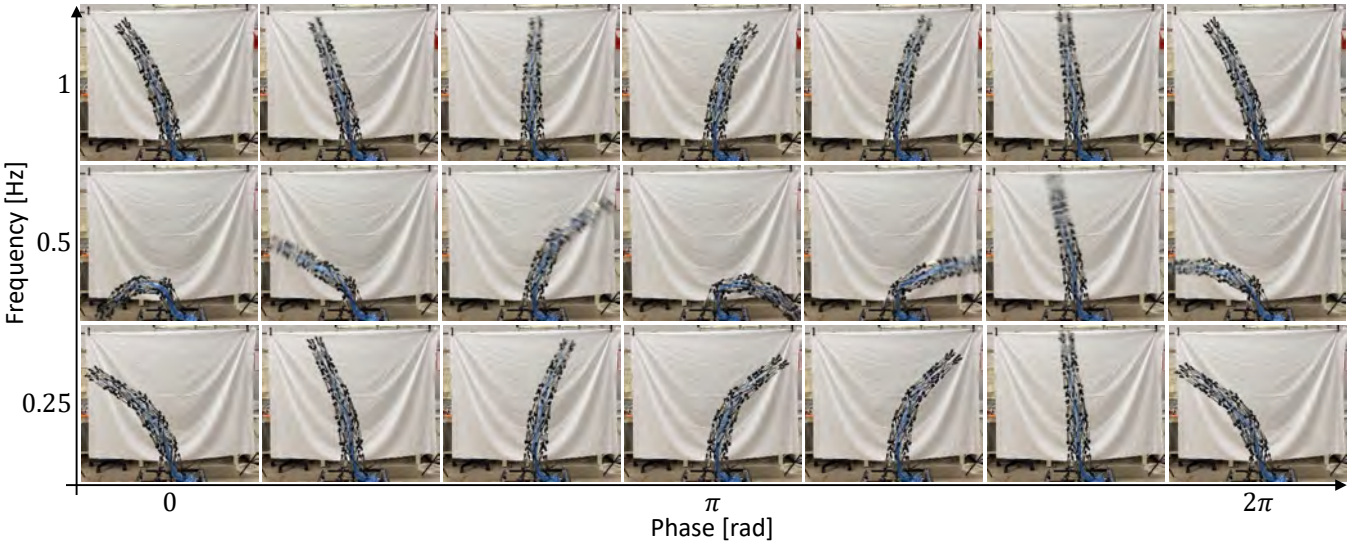

Fig. 11. Sequentially snapshots of one period of swing motions with different frequencies.

swing motions measured by a motion capture system (OptiTrack). The motion capture system can measure 3D positions of the tip, but we focus on the X-Y positions for analysis. As shown in this figure, the tip draw ellipsoidal trajectories in the X-Y plane. Torsion in each segment influences the ellipsoidal trajectories because torsion causes unexpected orthogonal displacement. To evaluate trajectories of swing motions, we apply Principal Component Analysis (PCA) and focus on the principal component 1.

Fig.10 shows changes in the contribution ratio of principal component 1. In this figure, the manipulator with springs exhibits a monotonic decrease of the principal component 1's contribution ratio corresponding to an increase in the input frequency. On the other hand, the developed manipulator exhibits turning to recovery of the contribution ratio around 1 [Hz] after the decreasing started around 0.5 [Hz]. Because the tensegrity manipulators have torsion in their structure, even if the pneumatic cylinders of each segment are grouped to the "Right" and "Left" to drive in opposite phases, the trajectory can be elliptical due to the unexpected orthogonal displacement. In addition, an increase in input frequency generally decreases the tip motion's amplitude. Therefore, Fig.10 means that the developed manipulator can reduce the unexpected orthogonal displacement thanks to the no-spring design.

Fig.11 shows sequential snapshots of one period of swing motions in the experiment. As already qualitatively seen in these snapshots, a wider swing happens at 0.5 [Hz] changes in desired pressures than the faster or the slower changes. It suggests that there is a resonant frequency in this system. To quantitatively evaluate the frequency response characteristics compared to that of the tensegrity manipulator with springs, we draw their Bode diagrams.

Fig.12 shows the Bode diagrams. As the upper plot of Fig.11 implies, a resonance can be found around 0.5 [Hz] as the local increase of gain. However, this feature appears

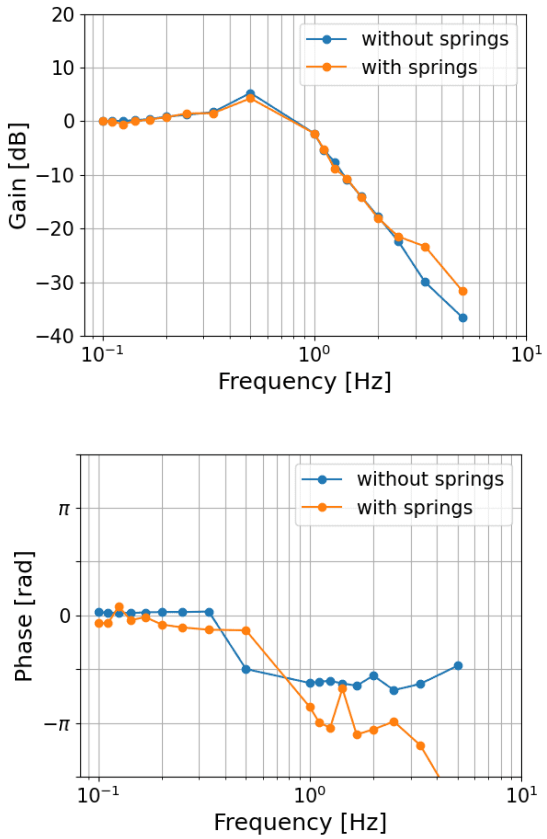

Fig. 12. The Bode diagrams of tensegrity manipulators with/without springs. Top: The gain plot. Bottom: The phase plot.

in both manipulators with/without springs. Therefore, it suggests that this resonance is mainly caused by a pneumatic actuation system consisting of pneumatic cylinders, air tubes, and pressure control valves which are commonly installed in both manipulators.

The difference between manipulators with/without springs

can be found in the lower plot of Fig.12. In this plot, at first, in contrast with that manipulator without springs does not exhibit delay less than approximately 0.5 [Hz], a manipulator with springs has a delay even in very slow movements. The use of stiffer springs may reduce this difference, but it also reduces the range of motion. In addition, increasing the stiffness of springs is not an effective solution because it is difficult to extend such a stiff spring during assembly. Therefore, it is considered an inherent drawback of installing springs in tensegrity robots.

Looking at the response above 0.5 Hz, a larger difference can be found. In contrast with that phase delay of the manipulator with springs keeps increasing according to increases in the input frequency, that of the manipulator without springs stays around $\pi/4$. It indicates that the structure of the manipulator without springs does not impose further delay and/or instability in contrast with the manipulator with springs.

IV. DISCUSSION

The experiments confirm the advantage of excluding mechanical springs from class 1 tensegrity robots. This section discusses design strategies that should be focused on in the future for tensegrity manipulators without springs.

Focusing on the sequential snapshots shown in the middle of Fig.11, it can be observed that there is a local large bending near the base. Such a large local bending causes a sudden decrease in bending stiffness, which can be a problem for control. When a pneumatic cylinder replaces a mechanical spring, it is difficult to reproduce the springiness at low loads due to the friction in cylinders, and thus this kind of problem is likely to occur. The developed tensegrity manipulator attempted to address this problem by using pneumatic cylinders of different diameters and a tapered shape. However, the large local bending means that they were insufficient.

There are two possible ways to solve this problem. The first way is to use struts with different lengths and different strokes pneumatic cylinders to enhance this attempt in the developed tensegrity manipulator. This will allow designing a more tapered shape without decaying the range of motion, and it eases the problem. The second way is to reconsider fixing a tensegrity structure to a base. Because the tensegrity does not rely on reaction force exerted from an environment, struts' three-dimensional displacements are possibly constrained by fixing the structure to a base. Although we tried to ease this issue by connecting the four strut ends of the tensegrity structure via four ball joints, it was insufficient. Adding sliders to add ball joins additional degrees of freedom will allow the connected struts more naturally incline, and thus the concentration of bending moment will reduce. Because these ways are not exclusive, including both improvements will be important future works of this study.

V. CONCLUSIONS

This paper presented a manipulator based on class 1 tensegrity consisting of 20 struts, 40 pneumatic cylinders, and 40 stiff cables. Because this manipulator has no mechanical springs in contrast with almost tensegrity robots, we expected improvements in strength and agility. Therefore, we conducted experiments to evaluate variable stiffness and frequency response. As a result, we could confirm the improvements comparing tensegrity manipulators with/without springs.

ACKNOWLEDGMENT

This work was supported by JSPS KAKENHI Grant Numbers 19K0285, 19H01122, and 21H03524.

REFERENCES

[1] R. E. Skelton and M. C. Oliveira, *Tensegrity Systems*. Springer Nature, 2009.

[2] C. Paul, F. J. Valero-Cuevas, and H. Lipson, "Design and control of tensegrity robots for locomotion," *IEEE Transactions on Robotics*, vol. 22, no. 5, pp. 944–957, 2006.

[3] J. Rieffel, J. R. Stuk, F. J. Valero-Cuevas, and H. Lipson, "Locomotion of a tensegrity robot via dynamically coupled modules," in *International Conference on Morphological Computation*, 2007, Conference Proceedings.

[4] M. Shibata and S. Hirai, *Rolling Locomotion of Deformable Tensegrity Structure*. WORLD SCIENTIFIC, 2009, pp. 479–486.

[5] K. Kim, A. K. Agogino, D. Moon, L. Taneja, A. Toghyan, B. Dehghani, V. SunSpiral, and A. M. Agogino, "Rapid prototyping design and control of tensegrity soft robot for locomotion," in *IEEE International Conference on Robotics and Biomimetics*, 2014, Conference Proceedings, pp. 7–14.

[6] A. Iscen, A. Agogino, V. SunSpiral, and K. Tumer, "Controlling tensegrity robots through evolution," in *Genetic and Evolutionary Computation Conference*, 2014, Conference Proceedings, p. 1293–1300. [Online]. Available: https://doi.org/10.1145/2463372.2463525

[7] M. Zhang, X. Geng, J. Bruce, K. Caluwaerts, M. Vespignani, V. SunSpiral, P. Abbeel, and S. Levine, "Deep reinforcement learning for tensegrity robot locomotion," in *IEEE International Conference on Robotics and Automation (ICRA)*, 2017, Conference Proceedings, pp. 634–641.

[8] P. Schorr, L. Zentner, K. Zimmermann, and V. Böhm, "Jumping locomotion system based on a multistable tensegrity structure," *Mechanical Systems and Signal Processing*, vol. 152, p. 107384, 2021.

[9] A. P. Sabelhaus, A. H. Li, K. A. Sover, J. R. Madden, A. R. Barkan, A. K. Agogino, and A. M. Agogino, "Inverse statics optimization for compound tensegrity robots," *IEEE Robotics and Automation Letters*, vol. 5, no. 3, pp. 3982–3989, 2020.

[10] D. Zappetti, R. Arandes, E. Ajanic, and D. Floreano, "Variable-stiffness tensegrity spine," *Smart Materials and Structures*, vol. 29, no. 7, p. 075013, 2020. [Online]. Available: http://dx.doi.org/10.1088/1361-665X/ab87e0

[11] S. Lessard, D. Castro, W. Asper, S. D. Chopra, L. B. Baltaxe-Admony, M. Teodorescu, V. SunSpiral, and A. Agogino, "A bio-inspired tensegrity manipulator with multi-dof, structurally compliant joints," in *IEEE/RSJ International Conference on Intelligent Robots and Systems*, Conference Proceedings, pp. 5515–5520.

[12] E. Jung, V. Ly, N. Cessna, M. L. Ngo, D. Castro, V. SunSpiral, and M. Teodorescu, "Bio-inspired tensegrity flexural joints," in *IEEE International Conference on Robotics and Automation*, Conference Proceedings, pp. 5561–5566.

[13] D. Fadeyev, A. Zhakatayev, A. Kuzdeuov, and H. A. Varol, "Generalized dynamics of stacked tensegrity manipulators," *IEEE Access*, vol. 7, pp. 63 472–63 484, 2019.

[14] S. Ikemoto, K. Tsukamoto, and Y. Yoshimitsu, "Development of a modular tensegrity robot arm capable of continuous bending," *Frontiers in Robotics and AI*, vol. 8, p. 347, 2021. [Online]. Available: https://www.frontiersin.org/article/10.3389/frobt.2021.774253